

# In-Situ UV Absorption $\text{CF}_2$ Sensor for Reactive Ion Etch Process Control

Hunsuk Kim and Fred L. Terry, Jr.

Department of Electrical Engineering and Computer Science  
University of Michigan, Ann Arbor, MI 48109-2122, USA

## ABSTRACT

In this article, we report the use of ultraviolet absorption spectroscopy for  $\text{CF}_2$  detection in a large area parallel plate capacitively coupled reactive ion etching system and correlation of data from this and other plasma sensors to the etch rate of  $\text{SiO}_2$  and  $\alpha$ -Si in  $\text{CF}_4/\text{CHF}_3$  plasmas. We present statistical models for estimation of  $\alpha$ -Si etch rate in the operational regime in which the  $\text{CF}_2$  concentration is in the range of 0.4 ~ 1.6 volume % of total gas in the etch chamber. A small change in  $\text{CF}_2$  concentration translates into quite a large variation in terms of  $\text{SiO}_2/\alpha$ -Si etch selectivity, and this makes  $\text{CF}_2$  concentration a useful variable in process control. We will show statistically that silicon etch rates can be very well estimated by using sensors for  $\text{CF}_2$  and fluorine.

**Keywords:** Reactive Ion Etching, Process Control,  $\text{CF}_2$  absorption sensor, statistical models

## 1. INTRODUCTION

It is commonly acknowledged that reactive ion etching (RIE) processes require empirical tuning on each etch tool to achieve desired wafer-level results and also require periodic adjustment to maintain high yields. Real-time feedback control could be used to reduce these problems provided that adequate plasma state sensors are available.<sup>1-3</sup>

Real-time RIE control requires simultaneous control of the chemical etch species, ion bombardment, and surface passivation mechanisms. Our previous work demonstrating the potential advantages of multi-variable feed control used only indicators of chemical species and ion bombardment.<sup>1</sup> In fluorocarbon-based processes, CF-polymer formation acts as the major surface passivation mechanism and has been shown to be related to the  $\text{CF}_2$  concentration in the plasma.  $\text{CF}_2$  is known to have absorption lines in ultraviolet range, and UV absorption spectroscopy is well suited to the RIE process both for its simplicity and non-perturbative nature.<sup>4</sup> We can also extract chamber wall state information from the  $\text{CF}_2$  sensor,<sup>5</sup> which is a sensitive indicator of etch performance. Combined with already used techniques such as reflectometry and actinometry, UV absorption spectroscopy for  $\text{CF}_2$  detection can be a very useful plasma state sensor intended for real-time RIE feedback control.

In this study, we show that UV absorption measurements of  $[\text{CF}_2]$  can be combined with actinometric measurement of relative  $[\text{F}]$  to build statistical models for  $\alpha$ -Si etch rates which are applicable to real-time feedback control. The plasma densities in this study are relatively low compared to other studies in the current literature,<sup>4,5</sup> but the  $\text{CF}_2$  detection still can be achieved with simple system requirements.

## 2. EXPERIMENT

A diagram of the apparatus used in this experiment is shown schematically in Fig. 1. The research vehicle is a Plasmatherm Clusterlock 7000 capacitively coupled parallel plate reactor. This machine is designed for etching flat panel display devices. This reactor accommodates 350 mm by 400 mm substrates, on which a few wafers can be placed and simultaneously processed. The chamber is of rectangular shape and there are five observation ports on each side. The UV grade quartz observation port windows allow 80% transmission at near 250 nm wavelength. The distance between opposing windows is 78 cm, and the width of the rf-biased rectangular electrode (along the observation line) is 61 cm. This electrode is connected to a 13.56 MHz rf generator and impedance matching network.

The light source of this absorption spectroscopy is a 100 W high pressure mercury arc lamp. To compensate the possible light source intensity level drift, we adopted the double beam technique. The light from the lamp is

---

Correspondence: F. L. Terry, Jr. Contact Information: F. L. Terry, Jr.; Email: fredty@eecs.umich.edu; Phone: 1-734-763-9764; Fax: 1-734-763-9324; Mailing address: 2408 EECS, 1301 Beal Ave., Ann Arbor, MI 48109-2122, USA. H. Kim; Email: hunsukim@eecs.umich.edu; Phone: 1-734-936-0971; Fax: 1-734-936-0347.

coupled to the common end of a bifurcated optical fiber. The light coming out from the two split ends are collimated and mechanically chopped at different frequencies. One of them is directly coupled to a 0.5 m monochromator with 1200 grooves/mm grating, which provides reference level of the light source, while the other beam is directed to a window, travels across the chamber, bounces back off the concave mirror installed on the other side of the chamber, travels back to the original departure window, and then enters the monochromator and converts into electrical signal through photomultiplier tube. Even though the collimated probe beam has a certain degree of divergence, due to the refocusing effect by the concave mirror, the beam diameter is not larger than 3 cm at all times. The reference and probe signals are recovered by phase-sensitive lock-in amplifiers synchronized with the optical chopper.

The gas mixture we use for the experiment is  $\text{CF}_4/\text{CHF}_3$ . The range of varying flow rate ratio is from  $\text{CF}_4 : \text{CHF}_3 = 1 : 3$  up to  $\text{CF}_4 : \text{CHF}_3 = 3 : 1$ . Total gas flow is fixed, which validates the assumption that for a given operating gas pressure the residence time of the gas species in the chamber is constant. There is 5 volume % argon included in  $\text{CF}_4$  gas feed for actinometry purposes. Emissions at 750.4 nm for Ar and at 703.7 nm for fluorine are measured and used to estimate relative concentration of fluorine.

For a highly polymerizing gas chemistry, it is often observed that polymerization on the windows reduces overall transmission light intensity even during the run, which makes it hard to distinguish the absorption by gas species in the chamber from the absorption by the coating polymer on the window. For etch rate measurement experiments, we checked the transmission level before and after the experiment and made sure that window absorption had reached steady state (“seasoned”). After confirming the chamber is properly seasoned for our operating conditions, we etched *a*-Si and/or  $\text{SiO}_2$  blanket wafers on 350 mm by 400 mm aluminum plate and collected etch rate information by SP microscopic reflectometry thin film thickness measurement after each run. We collected sensor data from  $\text{CF}_2$  absorption sensor and actinometry during the run.

### 3. RESULTS AND DISCUSSION

First, we scanned the monochromator from 245 nm through 254 nm wavelength range and verified the  $\text{CF}_2$  signature.<sup>6,7</sup> There are 3 major absorption peak in this wavelength range; 246 nm, 249 nm, and 252 nm, which have absorption cross-section of  $2.46 \times 10^{-17} \text{cm}^2$ ,  $2.91 \times 10^{-17} \text{cm}^2$ , and  $2.48 \times 10^{-17} \text{cm}^2$ . Once the peak location is verified,

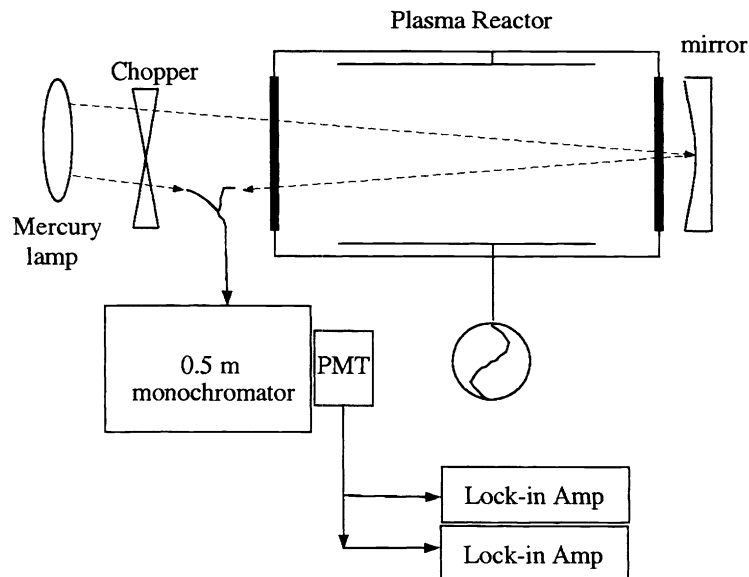


**Figure 1.** Schematic of the system used in this experiment.

we can fix the monochromator at that wavelength and measure the amount of absorption to get  $CF_2$  density. The density of  $CF_2$  ( $n$ ) is calculated by the Beer-Lambert relationship,

$$n = \frac{1}{\sigma b} \ln \left( \frac{I_0}{I} \right), \quad (1)$$

where  $\sigma$  is the absorption cross-section of  $CF_2$  at a given wavelength,  $b$  is the optical path length, and  $I$  and  $I_0$  are the transmitted probe beam intensity with and without the plasma on. This relationship assumes that the  $CF_2$  molecules are uniformly distributed across a certain distance along the optical path. Since the beam diameter is small enough compared to the size of the chamber height and electrode dimensions, and the electrode area is less ion confining than inductively coupled high density plasma which confines more discharge in center magnetic bucket area, it is reasonable to assume that in our reactor  $CF_2$  is distributed quite uniformly. With this assumption, the optical path length for this experiment is 156 cm ( $2 \times$  distance between opposing windows), and this gives lower limit of the density.

Fig. 2 shows typical  $CF_2$  absorption intensity observed at 252 nm wavelength as well as the percentage of the total gas under various operation conditions. Natural log of  $I_0/I$  is plotted against RF power for a few different pressures, which is proportional to  $[CF_2]$ . We see more absorption with increasing power and pressure as expected. But the partial pressure of  $CF_2$  decreases as the total gas pressure goes up. With the values given above and Eq. 1, the  $CF_2$  density in this plot is in the range of  $2.6 \times 10^{13} \text{ cm}^{-3} \sim 7.0 \times 10^{13} \text{ cm}^{-3}$ . For 40 mT total gas pressure, the volume % of  $CF_2$  is from 1.9 % to 4.4 %, while it is only from 1.3 % to 2.2 % for 100 mT in the RF power range from 200 W to 1100 W.

Fig. 2 is the result when we use a conventional glass plate as a wafer carrying tray. We put a plate inside the chamber when the plasma is turned on even if wafers are not loaded, to prevent the ion bombardment damage to the powered electrode. But with this glass plate inside, the  $V_{bias}$  reading does not reflect an actual self-bias voltage maintained in the sheath in front of the wafers inside the chamber. We have noticed that glass plate  $V_{bias}$  reading varies significantly according to the degree of polymerization in the chamber during the etch process. The  $V_{bias}$  reading decreases while the chamber is being coated with polymer, and the reading increases when the coated polymer is being removed during chamber cleaning. This is because the coated polymer on the electrically floating glass plate functions as a capacitor connected to the  $V_{bias}$  reading circuit in series. While ion charged on the polymer

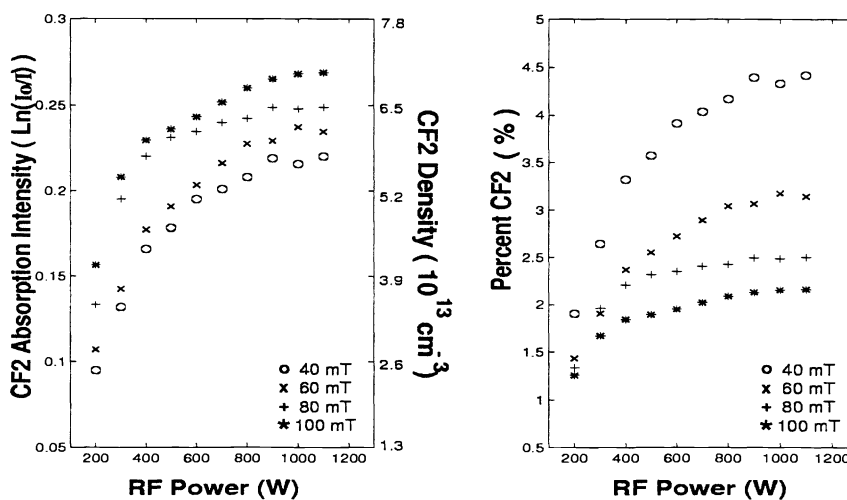


**Figure 2.**  $CF_2$  densities and percentage of total gas in various operating conditions.  $CHF_3$  plasma, 200 sccm gas flow, 252 nm absorption line.

film surface does not change drastically, increasing polymer thickness decreases the capacitance of the film, which in turn increases the voltage sustained by the polymer film capacitor. Therefore, voltage across the  $V_{bias}$  reading circuit reduces.

This phenomenon makes  $V_{bias}$  information provided by the Plasmatherm less useful when we try to correlate  $V_{bias}$  to ion flux. To get relevant  $V_{bias}$  information without placing another sensor in the chamber, we used an aluminum plate instead of glass, which provides direct electrical contact between electrode and plasma ambient. With this conducting plate in the chamber,  $V_{bias}$  reading stays constant during the run regardless of the degree of polymerization in our operational regime, and this gives a relevant information on dc self-bias in the plasma chamber. A typical set of experimental data is shown in Fig. 3. For the data presented in Fig. 3 and below, we used 249 nm absorption line. Wafers are etched for 3 minutes, and during this period sensor readings stay stable.

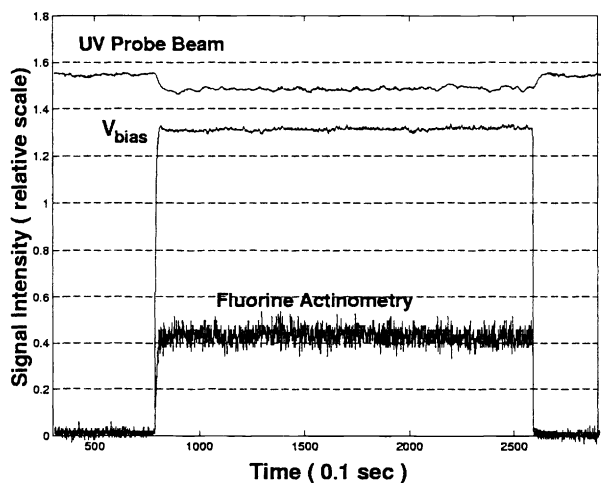


**Figure 3.** An example of raw data for a UV absorption experiment. The UV signal reduction when the plasma is on is about 3.8 %, which translates into 0.65%  $CF_2$  in the total gas mixture. The pressure was 40 mT, the rf power was 200 W, and the  $CF_4/CHF_3$  flow rate ratio was 3 : 1.

$CF_2$  is also a very sensitive indicator of etch selectivity between  $SiO_2$  and  $\alpha$ -Si. The etch rate change shown in Fig. 4 is measured under a fixed 40 mT, 500 W operation condition, while  $CF_4/CHF_3$  flow rate ratio changes. When pressure and RF power are fixed,  $V_{bias}$  is also fixed. This is the etch condition where the etch rate change is limited by the fluorine concentration. As the  $CF_2$  density increases, the  $SiO_2$  etch rate slowly decreases but the  $\alpha$ -Si etch rate quadratically decreases. In this set of experiments,  $CF_2$  density varies from  $1.2 \times 10^{13} \text{ cm}^{-3}$  to  $1.8 \times 10^{13} \text{ cm}^{-3}$ , which corresponds to the range of 0.9 ~ 1.4 % of total gas. About 60% change in  $CF_2$  sensor signal results in etch selectivity change by more than factor of 7.

We now try to extract statistical models from our data set to correlate the sensor information to the actual etch performance of the reactor. At a fixed pressure, by controlling RF Power and gas mixture we acquire information on  $CF_2$  concentration, fluorine concentration,  $V_{bias}$  and silicon etch rate. A statistically obtained model is not unique, and the choice of a specific model to describe a given data set is up to the user's discretion, considering statistical reliability as well as physically meaningful relationship between variables and end result.

We collected a data set to analyze under the condition of a fixed pressure at 40 mT and a fixed total gas flow rate. The etched material is amorphous silicon blanket wafer grown by PECVD. Again, the gas flow ratio between  $CF_4$  and  $CHF_3$  varies from 1:3 to 3:1, and the RF power varies from 150 W up to 600 W. The selected operation set points are evenly spaced in this gas flow ratio and RF power range so that the statistical weight does not concentrate in a specific region of the data space. Total of 22 experiments were performed, and for each experiment,  $[CF_2]$ ,  $[F]$ ,  $V_{bias}$  as well as etch rate data were collected.

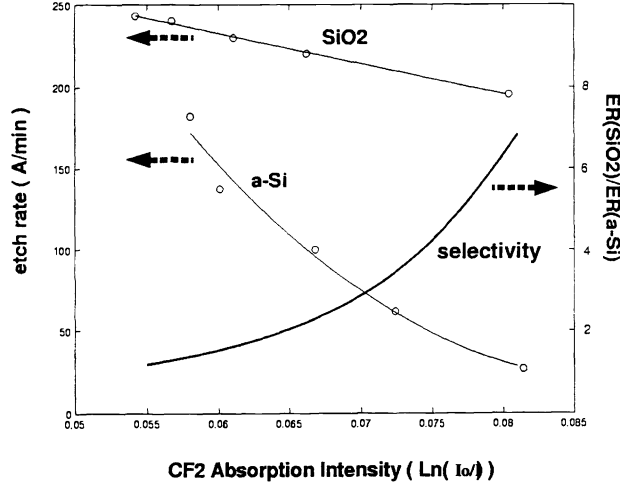


Figure 4.  $[CF_2]$  dependence of the  $SiO_2/a$ -Si etch selectivity when  $V_{bias}$  is maintained constant.

We present six models to describe the data set :

$$\begin{aligned}
 \text{model 1 : } ER &= -0.796 + 1.079 CFR + 0.814 Pw \\
 \text{model 2 : } ER &= -0.971 + 1.108 CFR + 0.992 V_{bias} \\
 \text{model 3 : } ER &= -0.390 + 0.505 CFR + 1.036 [F] \\
 \text{model 4 : } ER &= -0.929 + 0.734 CFR + 0.639 [F]^2 + 1.764 V_{bias} - 0.979 V_{bias}^2 \\
 \text{model 5 : } ER &= -0.399 + 1.253 [F] + 1.215 [CF_2] - 1.369 [CF_2]^2 \\
 \text{model 6 : } ER &= -0.891 + 0.481 CFR + 0.991 [F] + 1.820 [CF_2] - 1.442 [CF_2]^2
 \end{aligned}$$

where  $ER$  is the etch rate of  $a$ -Si,  $Pw$  is the applied RF power of the set point, and  $CFR$  is the partial pressure fraction of  $CF_4$  in  $CF_4/CHF_3$  gas mixture, i.e. for  $CF_4 : CHF_3 = 3 : 1$ ,  $CFR = 0.75$ , for  $CF_4 : CHF_3 = 1 : 3$ ,  $CFR = 0.25$ , etc. Quantities in the bracket  $[ ]$  are the densities of the species of interest measured by UV absorption sensor and actinometry system.

These models are obtained by standard least squares model fitting.<sup>8</sup> All the variables are normalized between 0 and 1 so that the coefficient of each term represents the influence of the variable in etch rate estimation. The range of actual values for the variables is in Table 1.

Table 1. The range of variable values before normalization.  $[CF_2]$  is in absorption intensity ( $\ln(I_0/I)$ ),  $[F]$  is in arbitrary units.

	min	max
CFR	0.25	0.75
Pw	150 W	600 W
$[CF_2]$	0.0254	0.0939
$[F]$	0.1001	0.5558
$V_{bias}$	94.0 V	319.3 V
ER	20 Å/min	239 Å/min

Each model is the best performance model with each set of variables while keeping only meaningful order terms. Sometimes we can achieve infinitesimal amount of improvement in the overall least square error by adding a number of higher order terms, but we have found variable terms with more than 3rd order do not play any statistically meaningful role in this particular estimation. A summary of fit table for these models is shown in Table 2. We can say that the model with smaller RMS\_error and larger RS\_Adj value is a better model. But this notion requires caution because we also have to take the physical reality into account.

With the gas pressure fixed at 40 mT, there are two degrees of freedom in setting the operation point:  $CF_4/CHF_3$  gas ratio and RF power. We know qualitatively that the silicon etch rate gets higher for higher powers and higher CFR's, which are closely related to ion bombardment enhanced etch/etchant formation and surface passivation inhibited etch behavior, respectively. Model 1 is an attempt to predict the etch rate by using only set point information, without any help from plasma state monitoring sensors. With  $RS\_Adj = 0.866$  and  $RMS\_error = 0.096$  (root mean square error, out of 0 to 1 scale), it certainly shows the etch rate trend we already know, but doesn't give us any new information let alone the accuracy the factory level process control requires.

In model 2,  $V_{bias}$  replaces Pw, and the fitting result gets better. This shows that even though  $V_{bias}$  is very much correlated to Pw ( $V_{bias} = 0.150 + 0.837 Pw$ ,  $RS\_Adj = 0.979$ ,  $RMS\_error = 0.03$ .),  $V_{bias}$  is a more directly related quantity to etch performance.  $V_{bias}$  can also be well estimated as a function of [F] and  $[CF_2]$  ( $V_{bias} = 0.010 + 0.688 [CF_2] + 0.631 [F]$ ,  $RS\_Adj = 0.941$ ,  $RMS\_error = 0.0504$ ).

The fitting quality experiences a boost when [F] replaces the position of  $V_{bias}$  in model 3. In this model, CFR reflects the degree of surface passivation inhibited etch behavior, and linear [F] term supports the established knowledge that chemical etching part of the Si etch rate is proportional to the fluorine density.<sup>9</sup> This shows that at least in this overall regime of operation set points, chemical etchant is more influential than ion bombardment enhancement etching.

It seems to be hard to point out any single individual physical etch mechanism from model 4. It is presented as a numerically best statistical model for our data set without the help of  $CF_2$  sensor, regardless of physical meanings. We couldn't get anything better than this without  $CF_2$  absorption sensor information. Model 4 serves as a baseline to show what benefit  $[CF_2]$  information can provide. It should be noted that absence in the formula does not mean the variable's irrelevance. Because of complex correlation between the variables, all models include effects from each variable to some extent. The task here is to find which set of variables represent the data set better and simpler.

In model 5,  $[CF_2]$  appears. The fitting performance of model 5 is slightly better than that of model 4, but the significance of this model is in that it achieves high correlation in etch rate estimation without the direct information of  $V_{bias}$ . We also put in  $V_{bias}$  as a variable, but with  $[CF_2]$  present,  $V_{bias}$  is eliminated in the fitting procedure. This model also explains the result shown in Fig. 4. Silicon etch rate quadratically decreases with  $[CF_2]$ . It linearly increases with [F]. Model 6 is the model 5 plus CFR. The result is the best of the six. Since CFR is always given as a set point parameter, the implementation of model 6 does not cost much more than model 5. By including a readily available parameter, we can limit the fitting space to more narrow and meaningful area.

**Table 2.** Fitting summary for etch rate estimation models. RS\_Adj estimates the proportion of the variation in the response around the mean that can be attributed to terms in the model rather than to random error. To make it more comparable over models with different number of parameters, RS\_Adj also uses the degrees of freedom in its computation.  $RS\_Adj = 1$  occurs when there is all-zero error perfect fit, while  $RS\_Adj = 0$  means that the fit predicts the response no better than the overall response mean. Mean response = 0.3324.

	RS_Adj	RMS_error
model 1	0.86586	0.09632
model 2	0.89582	0.08489
model 3	0.93827	0.06534
model 4	0.96749	0.04742
model 5	0.97296	0.04325
model 6	0.98234	0.03495

Fig. 5 is the comparison between actual *a*-Si etch rate from the experiments and predicted etch rate by model 6. All 22 points are shown. This is to show how well the statistical model predicts the etch rate. Fig. 6 includes contours for a few constant [F] values. A few contour lines ([F] = 0.1 ~ 0.45 (relative scale)) are shown. Model 5 and 6 indicates that for a constant [F], the silicon etch rate quadratically decreases as a function of [CF<sub>2</sub>].

#### 4. CONCLUSION

UV absorption spectroscopy for CF<sub>2</sub> detection can be used in conjunction with fluorine actinometry to predict etch rates for a wide range of operation condition. In the set point regime used in this experiment, the silicon etch rate varies by more than a factor of 11, and etch selectivity between silicon and oxide varies by more than a factor of 8. A Small change of CF<sub>2</sub> density results in large variation in etch rate, and the phase sensitive lock-in detection scheme has a sufficient resolution to pick up this change in CF<sub>2</sub> density.

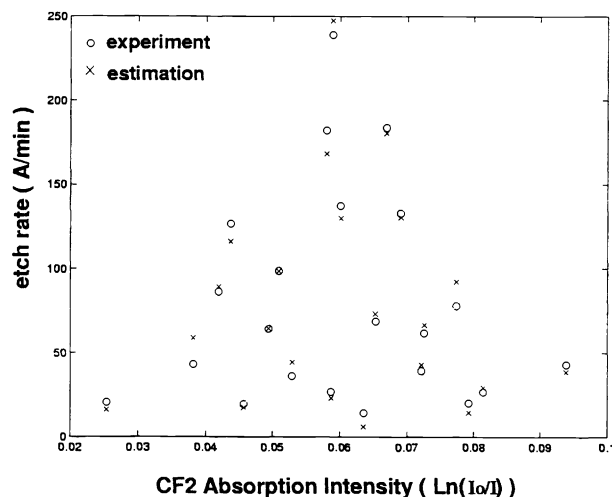


Figure 5. *a*-Si etch rate estimation by model 6.

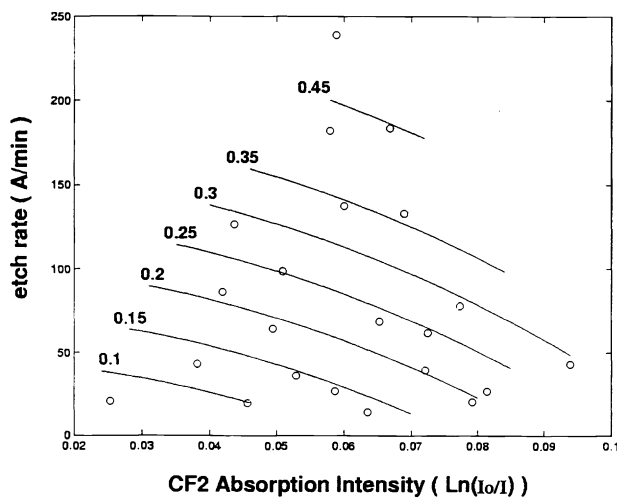


Figure 6. A Contour plot with [F] as a parameter. Experimental data points are denoted by small circles.

Even though ion bombardment enhancement, chemical etchant and surface passivation mechanism are all important factors determining silicon etch rate, second order polynomial of  $[CF_2]$  can fill in the absence of dc self-bias information to a certain extent. Highly confident statistical etch rate estimation model showing less than 3.5 % root mean square error has been presented.

It requires further study to find what kind of information  $[CF_2]$  can give in more extreme conditions, where either physical or chemical etch mechanism is dominant.

### ACKNOWLEDGMENTS

This work is supported in part by AFOSR/DARPA MURI Center for Intelligent Electronics Manufacturing (AFOSR F49620-95-1-0524) and the State of Michigan Center for Display Technology and Manufacturing. The authors would also like to thank Pete I. Klimecky for the assistance with the reactor operation and Kareemullah Khan for the assistance with statistical models.

### REFERENCES

1. B. A. Rashap, M. E. Elta, H. Etemad, J. P. Fournier, J. S. Freudenberg, M. D. Giles, J. W. Grizzle, P. T. Kabamba, P. P. Khargonekar, S. Lafortune, J. R. Moyne, D. Teneketzi, and F. L. Terry, Jr., "Control of semiconductor manufacturing equipment: real-time feedback control of a reactive ion etcher," *IEEE Trans. Semiconductor Manufacturing* **8**, pp. 286–297, 1995.
2. P. D. Hanish, J. W. Grizzle, M. D. Giles, and F. L. Terry, Jr., "A model-based technique for real-time estimation of absolute fluorine concentration in a  $CF_4/Ar$  plasma," *J. Vac. Sci. Tech. A* **13**, pp. 1802–1807, 1995.
3. N. Hershkowitz and H. L. Maynard, "Plasma characterization and process-control diagnostics," *J. Vac. Sci. Tech. A* **11**, pp. 1172–1178, 1993.
4. J. A. O'Neill and J. Singh, "Ultraviolet absorption spectroscopy for the detection of  $CF_2$  in high-density plasmas," *J. Appl. Phys.* **76**, pp. 5967–5974, 1994.
5. J. A. O'Neill and J. Singh, "Role of the chamber wall in low-pressure high-density etching plasma," *J. Appl. Phys.* **77**, pp. 497–504, 1995.
6. S. Sharpe, B. Hartnett, H. S. Sethi, and D. S. Sethi, "Absorption cross-section of  $CF_2$  in the  $\tilde{A}^1B_1-\tilde{X}^1A_1$  transition at 0.5 nm intervals and absolute rate constant for  $2CF_2 \rightarrow C_2F_4$  at  $298 \pm 3$  K," *J. Photochem.* **38**, pp. 1–13, 1987.
7. J.-P. Booth, G. Cunge, F. Neuilly, and N. Sadeghi, "Absolute radical densities in etching plasmas determined by broad-band UV absorption spectroscopy," *Plasma Sources Sci. Tech.* **7**, pp. 423–430, 1998.
8. *JMP: Statistical Software, ver. 3*, SAS Institute, Inc., Cary, NC, USA, 1998.
9. Y. H. Lee and M.-M. Chen, "Silicon etching mechanism and anisotropy in  $CF_4 + O_2$  plasma," *J. Appl. Phys.* **54**, pp. 5966–5973, 1983.